Nematic Main Chain Polymers with Head-to-Tail Structure: Synthesis and Enhanced NLO Response

C. Heldmann and M. Warner*

Cavendish Laboratory, Madingley Road, Cambridge CB3 OHE, U.K.

Received November 14, 1997; Revised Manuscript Received February 17, 1998

ABSTRACT: NLO-active semiflexible main chain polymers with a head-to-tail structure were synthesized from 2-nitro-4-carboxy-4′-[*N*-(11-hydroxyundecyl)-*N*-methylamino]azobenzene (CHRI) and 4-carboxy-4′-[*N*-(11-hydroxyundecyl)-*N*-methylamino]azobenzene (CHRII). The CHRI polymers, with molecular weight approximately 40 000, were not liquid crystalline. The electrooptical coefficient difference $r_{33} - r_{13}$ ranged between 0.75 and 1.36 pm/V depending on the particular sample. Theory suggests that nematic head-to-tail polymers can exhibit greatly enhanced electrooptical (EO) response. The 50/50 copolymers from CHRII and *p*-hydroxybenzoic acid (molecular weight 38 000) were liquid crystalline. $r_{33} - r_{13}$ was enhanced by up to a factor of 20 to $r_{33} - r_{13} \sim 21$ pm/V, with a comparable poling field around 8×10^6 V/m. The corresponding $\chi^{(2)}$ are around 62 pm/V. The dynamics of the induction of NLO response by a poling field was clearly high polymer-like. Relaxation of the EO response below T_g is imperceptible. Considering the smaller hyperpolarizability and lower number density of CHRII (compared to in the CHRI polymer), this enhancement is effectively ×40. Powerful chromophores, less modest poling fields, and longer chains should yield much larger $\chi^{(2)}$ using such polymers.

Introduction

Polymeric materials are attractive candidates for incorporation into nonlinear optical (NLO) devices.[1] This can be attributed to the relative ease with which they can be synthesized and processed. The wide variety of strategies[2] in the design and synthesis of NLO-active polymers all employ noncentrosymmetric molecules with a conjugated π-system as the basic building unit on the molecular level. The π-system is generally substituted with an electron donor at one end and an electron acceptor at the other end. However, the ways in which these NLO chromophores are incorporated into the polymeric material differ considerably. The most basic concept is to dissolve the guest NLO chromophores in a host polymer. Since the nonlinear optical response requires a noncentrosymmetric arrangement of the chromophores, the molecules have to be aligned in an electric field (the so-called poling process). Unfortunately, relaxation of the noncentrosymmetric order occurs even at temperatures well below (T_g − 50 °C) the glass transition temperature T_g.[3] Light scattering due to small crystals formed in the films of the material at higher concentration,[4] low solubility of the chromophores in the polymer matrix, and slow evaporation of the NLO-active molecules from the films[5] were other limiting factors.

Low solubility and phase separation of guest and host can be avoided by attaching the chromophore to the polymer chain. This gives rise to side chain[6] (commonly used for NLO[7]) and main chain polymers. In the first class, the chromophore is pendant to the backbone, connected via a more or less flexible (often alkyl) spacer. The class can be further divided according to whether the backbone is flexible (acrylates give good examples, for instance, in the context of NLO[7]) or rigid (e.g., fully aromatic polyesters).[8,9] With flexible backbones, the relaxation of the poled order and hence loss of the NLO response is mostly governed by the T_g associated with backbone motion. Therefore, most attempts to enhance the long-term stability of the material also increase the T_g of the polymer. When the polymer chain is rigid, the NLO properties are changed and the relaxation behavior is somewhat improved.[10,11] With the chromophore rigidly attached (without a flexible spacer) to a rigid rod-like main chain, the long term stability as well as the NLO response are drastically enhanced. The relaxation is no longer coupled with the glass transition temperature.

In this paper we present the synthesis, characterization, and the initial investigation of the nonlinear optical properties of a new polymeric material. It is of the second class, where the NLO-active chromophore is incorporated into the main chain rather than being pendant to a backbone. There have been several attempts to exploit the MC idea, most notably by Williams,[12−14] whose work is discussed below. It is important to stress that the polymer reported here is head-to-tail, e.g. all dipoles of the chromophores point in the same direction along the polymer backbone. This building principle leads to some synthetic constraints discussed in the synthetic part of this paper. Other groups have looked for MC polymers in a variety of ways: with flexible connectors,[15] as random polymers[16] (and have achieved high responses[17]), by polymerizing poled monomers,[18] and by taking a range of synthetic strategies; see for instance the work of Stenger-Smith *et al.*[19] and references contained therein.

It has been envisaged, for large rigid rod polymers[20] and for flexible main chain polymers,[12−14] that the head-to-tail arrangement of dipoles and chromophores along the main chain must lead to a considerable enhancement of NLO response and long term stability.

Consider first the rigid rod case, Figure 1, in a simplified form: each monomer, were it in a monomer liquid, would have a volume v, dipole moment μ, and hyperdipole β (with μ and β for simplicity directed along

* To whom correspondence should be sent.

S0024-9297(97)01693-8 CCC: $15.00
Published on Web 05/02/1998

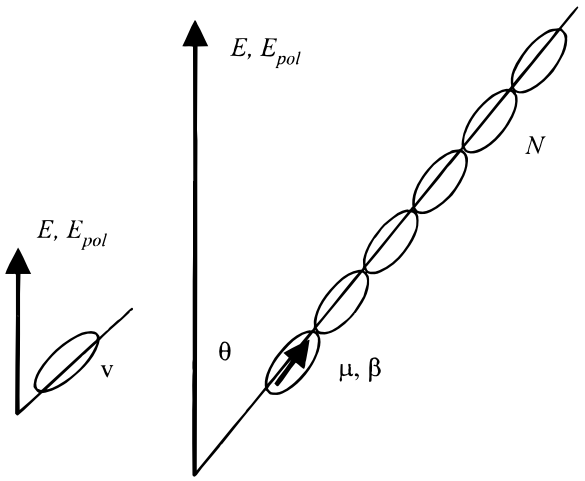

Figure 1. Ordering of short and long rods in an electric field. A short rod (single monomer) and an N-mer rod composed of the same monomers. Each monomer has a dipole and hyperdipole (μ and β) which in the case of the polymer point coherently along the chain backbone. Each monomer has a volume v. Both the short and long rods are shown at an angle θ to the optical and poling fields (E and E_{pol}).

the rod axis). Such a liquid would have, for instance, a second-order response along the field direction of

$$\chi^{(2)}_{333} = \frac{\beta}{v}\langle\cos^3\theta\rangle \qquad (1)$$

where β/v is the hyperdipole per unit volume and $\langle\cos^3\theta\rangle$ accounts for the average projection factor between the electric field E of the light wave and the axes of the molecules. This average is non zero if the system is poled—an applied electric field E_{pol} biases the molecules so that more are parallel than antiparallel to it (centrosymmetry is broken). In an isotropic[21a] system the average is[21b] $\langle\cos^3\theta\rangle = \mu E_{pol}/5k_BT$; the poling field, if not too large, creates a small bias since the dipolar energy μE_{pol} is in competition with the rods' thermal disordering (with energy scale k_BT at temperature T associated with their random orientations). A longer rod has the same hyperdipole density β/v and the same thermal energy k_BT. The dipolar bias energy, however, is now $N\mu E_{pol}$, if there are N monomers and hence N dipoles per rod, and the dipolar order is correspondingly greater: $\langle\cos^3\theta\rangle = N\mu E_{pol}/5k_BT$. The $\chi^{(2)}_N$ of the N-mer is thus $N\chi^{(2)}_1$, where $\chi^{(2)}_1$ would be the NLO response of a fluid of the monomers. Depending on the molecular weight and stiffness of the polymer chain, this enhancement can be expected to be in the range of up to several orders of magnitude and was first experimentally verified by EFISH measurements of poly(benzyl glutamate) (PBLG) in ethylene dichloride by Levine *et al.*[20] PBLG approximates a long, unbending rod. In considering the actual fields acting on the hyperdipole β and the dipole μ, we have ignored the subtle problem of internal field corrections. Whether in simple or in polymeric fluids, these differ by factors from the fields applied to the sample. We absorb all such factors into β and μ, which are then effective (hyper)dipoles.

Semiflexible polymers with the coherent dipole architecture should also give an enhancement.[12−14] They are locally stiff, and those monomers within a persistence length of each other (C_∞ in number in Flory's notation[22]) effectively act as a single unit. We thus have instead for the average order in the above $C_\infty\mu E_{pol}/5k_BT$ and hence $\chi^{(2)}_N = C_\infty\chi^{(2)}_1$: the enhancement is no longer extensive in the chain length. A limited enhancement has been seen by Williams *et al.*[12−14] in isotropic polymer melts.

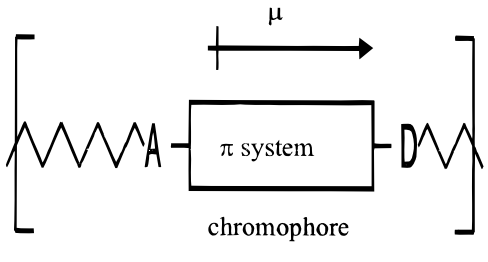

Figure 2. Schematic representation of the structure of a semiflexible main chain with a head-to-tail arrangement of chromophores and semiflexible spacers along the backbone.

In a certain sense the above results, though successful, are also disappointing. Stiff rods order nematically[20] and, in the case of PBLG also gel, if the concentration is too high. Both effects impede the dynamics of up−down ordering required to form the bias demanded by E_{pol}. Avoiding the problem by dilution also reduces the number density of chromophores and hence $\chi^{(2)}$. There is still an enhancement by a factor of N over a system of monomers at the same weight concentration, but the $\chi^{(2)}$ is still so small it is not useful for device applications. On the other hand if one increases the stiffness in the Williams systems to get more dipoles acting cooperatively (a large C_∞), then there are log jams and/or strong nematic order that impedes the buildup of the poled state.

The alternative[23−25] is to take head-to-tail polymers of very limited stiffness but nevertheless composed of rods concatenated along the backbone and of sufficient length such that a nematic phase is formed. The flexibility stems from the spacers at each end of the rods that connect them to neighboring rods along the backbone. The schematic requirements of the building blocks are shown in Figure 2.

The nematic order (shown in Figure 3) then causes the component parts of the chain to be nearly (depending on the strength of the order) up or down the nematic field.

Reversals of direction necessitate bending the spacer and locally violating the nematic field. If the flexibility, nematic order, and the length of the rods are appropriately adjusted, then the reversals become sufficiently rare and well defined that one could think of them as hairpins.[26] In this limit, and correspondingly less so at lower order, the chain becomes extended along the nematic direction—larger and larger sections of chain act cooperatively. This mechanism for chain extension has been seen directly by neutron scattering.[27] Our first purpose in this paper is to inquire as to whether an enhancement in $\chi^{(2)}$ corresponding to the change in chain dimension can be seen in going from the isotropic to nematic analogue. The coherent unit (Figure 3) has in effect a dipole a factor of l_{step}/l_{mon} greater than that of a monomer (this factor is the analogue of C_∞ for the nematic state), and the dielectric response should be enhanced by the same factor. This mechanism for the enhancement of $\chi^{(1)}$ and $\chi^{(2)}$ has been explored theoretically in some detail.[23,24] One requires flexibility sufficient to allow chain reversals, but not so small that coherence between consecutive dipoles is lost altogether. The predicted dielectric response enhance-

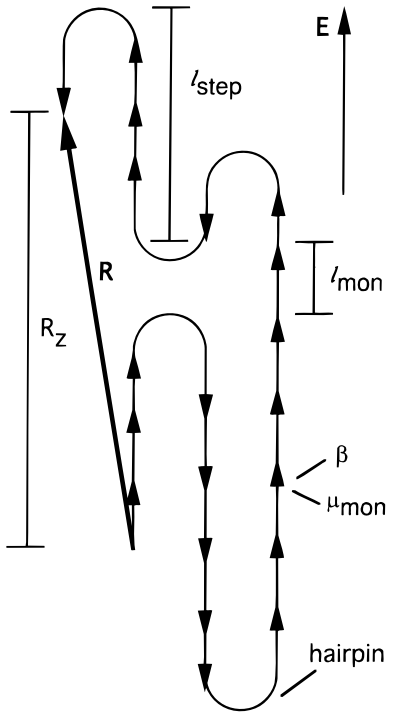

Figure 3. Schematic representation of a head-to-tail polymer in an electric poling field. Note that changes in direction represent the boundaries of regions in the chain with oppositely directed dipoles and hyperdipoles.

ment ranges from a factor of the degree of polymerization N (when hair pins are rare and the chain is stretched out) to a factor of 1 as the chains have joints flexible enough they behave like the corresponding monomeric fluid.

Are there barriers to the achievement of the poled state? Unlike with long rigid rods, the individual chains can turn over without the necessity to turn bodily. In Figure 3 it is clear that the regions of chain reversal are mobile and give a mechanism, via their motion, of turning over the constituent dipoles (and hyperdipoles) of the chain without impediment by the nematic field or by log jams. When order is high, one can think of this response as via the motion of hairpins that leave a wake of turned over chain as they move.

As in all high polymers, motion of the whole chain relies on the motion of many constituent parts and is characteristically slow, perhaps even seconds, but is not impossible. On the other hand, quenching below T_g stops gross chain motion. Local motion, however, persists, a mechanism by which poled order is still able to decay in SC nematic polymers. Poled order in MC nematics, dependent as it is nongross motion, does not seem to have a decay mechanism in the glassy state. Our second two purposes are thus to look for high polymer dynamical response to poling and to investigate the complete temporal stability of quenched poled polymers.

We shall first describe the synthesis of polymers that meet the subtleties of structure discussed above and then address their characterization. We then discuss the details and difficulties associated with $\chi^{(2)}$ measurements and indicate how these problems will be addressed in future work. Here we are not interested *per se* in ultrahigh $\chi^{(2)}$ values—the small hyperpolarizabilities and poling fields we employ preclude this—but are rather concerned with the enhancement associated with MC nematic polymers. In fact, the values we report compare favorably with those of the literature, but it is the enhancement that gives hope for very high future values by this route.

Experimental Section

Column Chromatography. All column chromatograms were run on glass columns using Merck Silica gel grade 60, 230-400 mesh, 60 Å. The solvents used are quoted in the individual recipes.

Thin Layer Chromatography (TLC). TLC chromatograms were executed on DC-Aluminiumfolien Kieselgel 60 F_{254} by Merck.

Infrared Spectroscopy (IR). IR spectra were recorded on a Nicolet 510 Fourier transform infrared spectrometer. The spectra were measured from KBr disks containing small amounts of the particular compound.

Nuclear Magnetic Resonance Spectroscopy (NMR). All proton (^{1}H) and carbon (^{13}C) spectra were recorded on a Bruker 250 MHz spectrometer with the solvent as internal standard.

Elemental Analyses. Elemental analyses were performed by the Microanalysis unit, Department of Chemistry, Lensfield Road, Cambridge, U.K.

Differential Scanning Microscopy (DSC). All thermograms were obtained with a Perkin-Elmer Delta Series DSC-7 with a nitrogen atmosphere and a cooling facility allowing temperatures down to −50 °C.

Microscopy. Mesophase transition temperatures were visualized using a Zeiss Axioscop polarizing microscope equipped with a Linkam TMS 91 hotstage controller, CS 196 cooling system, and VTO 232 video facilities.

Solvents. Solvents were used as obtained except for solvents that were used in polycondensations. Dichloromethane was dried over calcium hydride and then distilled. Dimethylformamide was dried over molecular sieves.

Film Preparation. Samples for the electrooptical measurements were prepared as follows: A 3-5% polymer−tetrahydrofuran or 1,1,2,2-tetrachloroethane solution was spin coated onto a glass slide that was covered with a conducting layer of ITO. Typical polymer film thicknesses obtained at a spinning rate of 800 rpm at room temperature were 0.2−0.5 μm (depending on the concentration of the solution and the type of solvent). The films were dried at room temperature and a several hundred nanometer thick aluminum top electrode was evaporated on top of the layered structure. The dried films were poled by applying an electric field between the ITO and aluminum electrodes.

Syntheses. *N*-(11-Hydroxyundecyl)-*N*-methylaniline (9) (See Scheme 2). A suspension of *N*-methylaniline (29.7 g, 0.28 mol), 11-bromoundecanole (70.0 g, 0.28 mol), potassium carbonate (57.8 g, 0.42 mol), and potassium iodide (1.75 g, 0.11 mol) in 175 mL of *n*-butanol was stirred for 4 days at 120−130 °C under nitrogen. The mixture was cooled to room temperature, the inorganic salt was filtered off, and the solvent was evaporated. Fractional distillation yields 42.7 g (56%) of an oily, usually slightly green liquid (bp ca. 170 °C at 0.5 mbar). ^{1}H-NMR ($CDCl_3$): δ = 1.33 (m, 14H, $N(CH_2)^{3-9}$), 1.58 (m, 4H, $N(CH_2)^2$, $HO(CH_2)^2$), 2.09 (s broad, 1H, OH), 2.95 (s, 3H, NCH_3), 3.33 (t, 2H, NCH_2), 3.63 (t, 2H, $HOCH_2$), 6.68 (m, 3H, H_2, H_3), 7.26 (m, 1H, H_1). ^{13}C-NMR ($CDCl_3$): δ = 25.8 ($N(CH_2)^9$), 26.7, 27.2, 29.481, 29.6, 29.6 ($N(CH_2)^{3-8}$), 32.8 ($N(CH_2)^2$, $N(CH_2)^{10}$), 38.3 (NCH_3), 52.9 (NCH_2), 62.9 (OCH_2), 112.3 (C_2), 116.0 (C_4), 129.1 (C_3), 149.4 (C_1). IR (cm^{-1}): 690 (m), 746 (m), 1034 (w), 1057 (w), 1368 (m), 1466 (m), 1506 (vs), 1599 (s), 2853 (s), 2927 (vs), 3340 (m, very broad).

4-Acetamidobenzoic Acid (2) (See Scheme 1). To a suspension of *p*-aminobenzoic acid (**1**) (50.0 g, 0.37 mol) in 100 mL of toluene was added acetic anhydride (55.9 g, 0.55 mol). The mixture was stirred (mechanical stirrer) at 130 °C. After 4 h the reaction mixture was cooled to room temperature, and the solid was filtered off, thoroughly washed with toluene, and dried under vacuum (80 °C). Yield: 58.6 g (89%). ^{1}H-NMR (DMSO-d_6): δ = 2.08 (s, 3H, $COCH_3$), 7.70 (d, 2H, H3), 7.94

(d, 2H, H2), 10.25 (s, 1H, NHCO), 12.69 (s broad, 1H, COOH). ^{13}C-NMR (DMSO-d_6): δ = 24.3 (CH_3), 118.3 (C_3), 125.0 (C_1), 130.5 (C_2), 143.5 (C_4), 167.1, 169.0 (NHCO, COOH). IR (cm^{-1}): 503 (w), 1263 (s), 1425 (m), 1522 (s), 1593 (m), 1672 (vs) 3307 (m).

4-Acetamido-3-nitrobenzoic Acid (3)[28] (See Scheme 1). A three-neck flask fitted with inner thermometer, dropping funnel, and mechanical stirrer was charged at room temperature with *p*-acetamidobenzoic acid (**2**) (18.5 g, 0.11 mol) and 30 mL concentrated sulfuric acid. The benzoic acid partially dissolved to form a very thick mixture. The suspension was cooled to 2−5 °C with an ice/salt bath, and a mixture of 16.1 mL of concentrated sulfuric acid in 29.3 mL of 65% nitric acid was added very slowly (1 h) to maintain the temperature in the given limits. After completion the ice/salt bath was replaced by an ice bath and stirred for another hour at 10 °C. The reaction mixture was poured into 350 mL of water containing a few pieces of ice. The pale yellow precipitate was filtered off, several times washed with water, dried under vacuum (60 °C), and recrystallized from ≈300 mL of 2-propanol/20 mL of water. Yield: 15.2 g (61%). ^{1}H-NMR (DMSO-d_6): 2.12 (s, 3H, CH_3), 7.82 (d, 1H, H5), 8.19 (dd, 1H, H6), 8.37 (d, 1H, H2), 10.55 (s, 1H, NH), 13.49 (s broad, 1H, COOH). ^{13}C-NMR (DMSO-d_6): 23.8 (CH_3), 124.6 (C5), 126.1 (C2), 126.9 (C1), 134.5 (C6), 135.2 (C4), 141.2 (C3), 165.4, 168.9 (NHCO, COOH). IR (cm^{-1}): 528 (s), 1254 (vs), 1479 (m), 1630 (s), 1688 (s), 3367 (m), 3480.87 (m).

4-Amino-3-nitrobenzoic Acid (4) (Scheme 1). A suspension of **3** (12.0 g, 0.054 mol) in 145 mL of concentrated hydrochloric acid (density: 1.18 g/mL) was stirred at 80 °C for 2 h. The mixture was poured onto 300 mL of ice water. The yellow precipitate was filtered off, washed with cold water, dried for 2 h under vacuum and stirred in 50 mL of ethyl acetate. The solid was filtered off and recrystallized from ethanol. Yield: 7.0 g (72%). ^{1}H-NMR (DMSO-d_6): 7.04 (d, 1H, H5), 7.85 (dd, 1H, H6), 7.94 (s, 2H, NH_2), 8.54 (d, 1H, H2), 12.81 (s, 1H, COOH). ^{13}C-NMR (DMSO-d_6): 117.6 (C1), 119.3 (C5), 128.2 (C2), 129.8 (C3), 135.3 (C6), 148.8 (C4), 166.12 (COOH). IR (cm^{-1}): 527 (w), 1252 (vs), 1630 (vs), 1690 (m), 3367 (m), 3481 (m).

2-Nitro-4-carboxy-4′-[*N*-(11-hydroxyundecyl)-*N*-methylamino]azobenzene (CHRI)[29] (Scheme 1). A solution of 56 mL of hydrochloric acid (5 mol L^{-1}) was cooled to 0 °C, and sodium nitrate (0.53 g, 7.71 mmol) in 7 mL of water was slowly added. 3-Nitro-4-aminobenzoic acid (**4**) (7.0 g, 38.5 mmol) was dissolved in a solution of sodium hydoxide (1.54 g, 38.5 mmol) in 58 mL of water and was then combined with a solution of sodium nitrate (2.80 g, 40.58 mmol) in 18 mL of water. This solution was slowly added under stirring to the hydrochloric acid solution so that the temperature was kept within 5−10 °C. At the end of the diazotization, a fine precipitate of the diazonium salt was formed. After complete addition the solution was allowed to stir for another 30 min and a spatula of urea was then added to destroy an excess of sodium nitrate. The prepared diazonium solution was then added at 5−10 °C to a solution of *N*-methyl-*N*-(11-hydroxyundecyl)aniline (**9**) (9.5 g, 34.2 mmol) in 70 mL of *p*-dioxane. The clear solution turned immediately red, and a precipitate was formed after a short time. After complete addition the mixture was stirred for another 30−45 min. Sodium acetate (3.0 g) and sodium chloride (6.0 g) and, after 20 min, 100 mL of water were added. The precipitate was filtered off, washed with water, and carefully dried in vacuum. The nearly black compound was recrystallized twice from toluene. A part of the material (5 g) was dissolved in a small amount of acetone (150 mL) and precipitated with 1 L of *n*-hexane. Yield: 9.2 g (57.3%). ^{1}H-NMR (DMSO-d_6): 1.21 (m, 14H, $(CH_2)^3(CH_2)^9$), 1.38 (quin, 2H, $(CH_2)^2$), 1.53 (quin, 2H, $(CH_2)^{10}$), 3.06 (s, 3H, NCH_3), 3.35 (t, 2H, NCH_2), 3.45 (t, 2H, $(CH_2)^{11}$), 4.33 (s broad, 1H, OH), 6.83 (d, 2H, H3′, H5′), 7.74, 7.77 (2 d, 3H, H5, H2′, H6′), 8.22 (dd, 1H, H6), 8.41 (d, 1H, H2), 13.60 (s broad, ≈1H, COOH). IR (cm^{-1}): 1115 (s), 1144 (vs), 1245 (m), 1312 (m), 1358 (m), 1431 (w), 1526 (w), 1600 (vs), 1684 (w), 2850 (w), 2925 (w). Anal. Calcd for ($C_{25}H_{34}O_5N_4$): C, 63.8; H, 7.3; N, 11.9; O, 17.00. Found: C, 63.6; H, 7.3; N, 11.8.

4-Carboxy-4′-[*N*-(11-hydroxyundecyl)-*N*-methylamino]-azobenzene (CHRII) (Scheme 3). A solution of sodium nitrate (3.0 g, 43.5 mmol) in 15 mL of water was added dropwise to a cooled solution (0−5 °C) of *p*-aminobenzoic acid (**1**) (5.5 g, 40.2 mmol) in 10.4 mL of concentrated hydrochloric acid and 33 mL of distilled water. After complete addition the solution was stirred for another 15 min and a spatula of urea was added to destroy an excess of sodium nitrate. This solution was added to *N*-methyl-*N*-(11-hydroxy undecyl)aniline (**9**) (10.1 g, 36.5 mmol) in 70 mL of *p*-dioxane. A deep red color appeared immediately, and after the addition of half of the diazonium solution, 6.0 g of sodium acetate was added. The color changed from red to orange. After another 30 min at 5 °C the slurry mixture was poured into 1.5 L of cold water that contained four spatulas of sodium acetate. The orange precipitate was filtered off, carefully dried under vacuum at 40 °C and recrystallized from toluene. Yield: 12.7 g (82%). ^{1}H-NMR (DMSO-d_6): 1.19 (m, 14H, $(CH_2)^3(CH_2)^9$), 1.38 (quin, 2H, $(CH_2)^2$), 1.49 (quin, 2H, $(CH_2)^{10}$), 2.99 (s, 3H, NCH_3), 3.36 (2t, 4H, NCH_2, $(CH_2)^{11}$), 4.35 (s broad, 1H, OH), 6.76 (d, 2H, H3′, H5′), 7.79, 7.82 (2 d, 4H, H2′, H6′, H2, H6), 8.08 (d, 2H, H4, H5), 13.07 (s broad, ≈1H, COOH). ^{13}C-NMR (DMSO-d_6): δ = 25.77 ($N(CH_2)^9$), 27.0, 26.5, 26.6, 29.1, 29.2, 29.3, 32.7 ($N(CH_2)^{2-10}$), 38.7 (NCH_3), 51.8 (NCH_2), 60.9 (OCH_2), 111.4 (C3′, C5′), 121.8 (C2, C6), 125.6 (C2′, C6′), 130.6 (C3, C5), 130.9, 142.6, 152.1, 155.3 (C4, C1′, C1, C4′), 167.1 (CO). IR (cm^{-1}): 540 (w), 1144 (vs), 1273 (m), 1385 (m), 1603 (s), 1690 (s), 2497 (w), 2854 (w), 2925 (m), 3438 (m, broad). Anal. Calcd for ($C_{25}H_{35}O_3N_3$): C, 70.6; H, 8.3; N, 9.9; O, 11.3. Found: C, 70.7; H, 8.4; N, 9.9.

Polycondensation (Typical Examples).[30] Four different types of polymers were prepared by polycondensation: CHRI, CHRII, CHRI plus HBA, CHRII plus HBA. In each case 2 mmol total of the hydoxy acid monomers and 1 mmol of the complex of PTSA·DMAP[30] were suspended under nitrogen in ca. 10 mL of dry dichloromethane. Diisopropylcarbodiimide (3 mmol) was added via syringe. Nearly instantaneously, the monomers CHRI and CHRII started to dissolve while a white precipitate of the urea derivative was formed. The reaction mixture was stirred at room temperature for 2−3 days and then poured into 120 mL of methanol. The precipitate was stirred in a mixture of 100 mL of methanol and 25 mL of dichloromethane, filtered off, and dried. The polymers were purified further by Soxhlett extraction with acetone or ethyl acetate. Yield: usually 50-80%.

Data for P1D. ^{1}H-NMR ($CDCl_3$): 1.28 (m, 14 H, $(CH_2)^3$-$(CH_2)^9$), 1.61 (quin, broad, 2H, $(CH_2)^2$), 1.79 (quin, 2H, $(CH_2)^{10}$), 3.05 (s, 3H, NCH_3), 3.41 (t, 2H, NCH_2), 4.32 (t, 2H, O-$(CH_2)^{11}$), 6.68 (d, 2H, H3′, H5′), 7.75 (d, 1H, H6), 7.85 (d, 2H, H2′, H6′), 8.21 (dd, 1H, H5), 8.42 (d, 1H, H3). Anal. Calcd for ($C_{25}H_{32}O_4N_4$): C, 66.4; H, 7.1; N, 12.4; O, 14.1. Found: C, 66.2; H, 7.3; N, 12.3.

Data for P2. ^{1}H-NMR ($CDCl_3$): 1.29 (m, 14H, $(CH_2)^3$-$(CH_2)^9$), 1.59 (m, 2H, $(CH_2)^2$), 1.78 (m, 2H, $(CH_2)^{10}$), 3.06 (s, 3H, NCH_3), 3.62 (t, 2H, NCH_2), 4.32 (t, 2H, $O(CH_2)^{11}$), 6.71 (d, 2H, H3′, H5′), 7.84, 7.90 (d, 4H, H2′, H6′, H2, H6), 8.13 (d, 2H, H3, H5). IR (cm^{-1}): 820 (w), 998 (w), 1053 (m), 1134 (vs), 1215 (m), 1272 (m), 1377 (s), 1514 (m), 1599 (s), 1709 (s), 1773 (m), 2850 (m), 2921 (m), 3369 (w). Anal. Calcd for ($C_{25}H_{33}O_2N_3$): C, 73.7; H, 8.2; N, 10.3; O, 8.9. Found: C, 73.8; H, 7.9; N, 10.2.

Data for [CHRII$_{0.75}$HBA$_{0.25}$]. ^{1}H-NMR ($CDCl_3$): 1.27 (m, 14H, $(CH_2)^3(CH_2)^9$), 1.59 (q, 2H, $(CH_2)^2$), 1.74 (q, 2H, $(CH_2)^{10}$), 3.02 (s, 3H, NCH_3), 3.37 (t, 2H, NCH_2), 4.30 (t, 2H, $O(CH_2)^{11}$), 6.69 (d, 2H, H3′, H5′), 7.30 (d, 0.48H, H3, H5, 4-HBA), 7.39 (d, 0.18H, H3, H5, 4-HBA), 7.81 7.83, 7.86 (2d, 4H, H2′, H6′, H2, H6), 8.10 (d, 2H, H3, H5), 8.26 (d, 0.68 H, 2H, 6H, 4-HBA). IR (cm^{-1}): 1054 (m), 1133 (s), 1198 (m), 1269 (m), 1312 (m), 1379 (m), 1515 (m), 1598 (vs), 1711 (s), 2850 (w, broad), 2921 (w, broad), 3419 (w, broad). Anal. Calcd for ($C_{20.5}H_{25.75}O_2N_{2.25}$): C, 73.4; H, 7.7; N, 9.4; O, 9.5. Found: C, 72.6; H, 7.6; N, 10.0.

Data for [CHRII$_{0.50}$HBA$_{0.50}$]. ^{1}H-NMR ($CDCl_3$): 1.31 (m, 14H, $(CH_2)^3(CH_2)^9$), 1.64 (m, 2H, $(CH_2)^2$), 1.77 (m, 2H, $(CH_2)^{10}$), 3.07 (s, 3H, NCH_3), 3.42 (t, 2H, NCH_2), 4.33 (t, 2H, $O(CH_2)^{11}$),

Scheme 1. Synthesis of 2-Nitro-4-carboxy-4′-[*N*-(11-hydroxyundecyl)-*N*-methylamino]azobenzene (CHRI) and polymer P1[a]

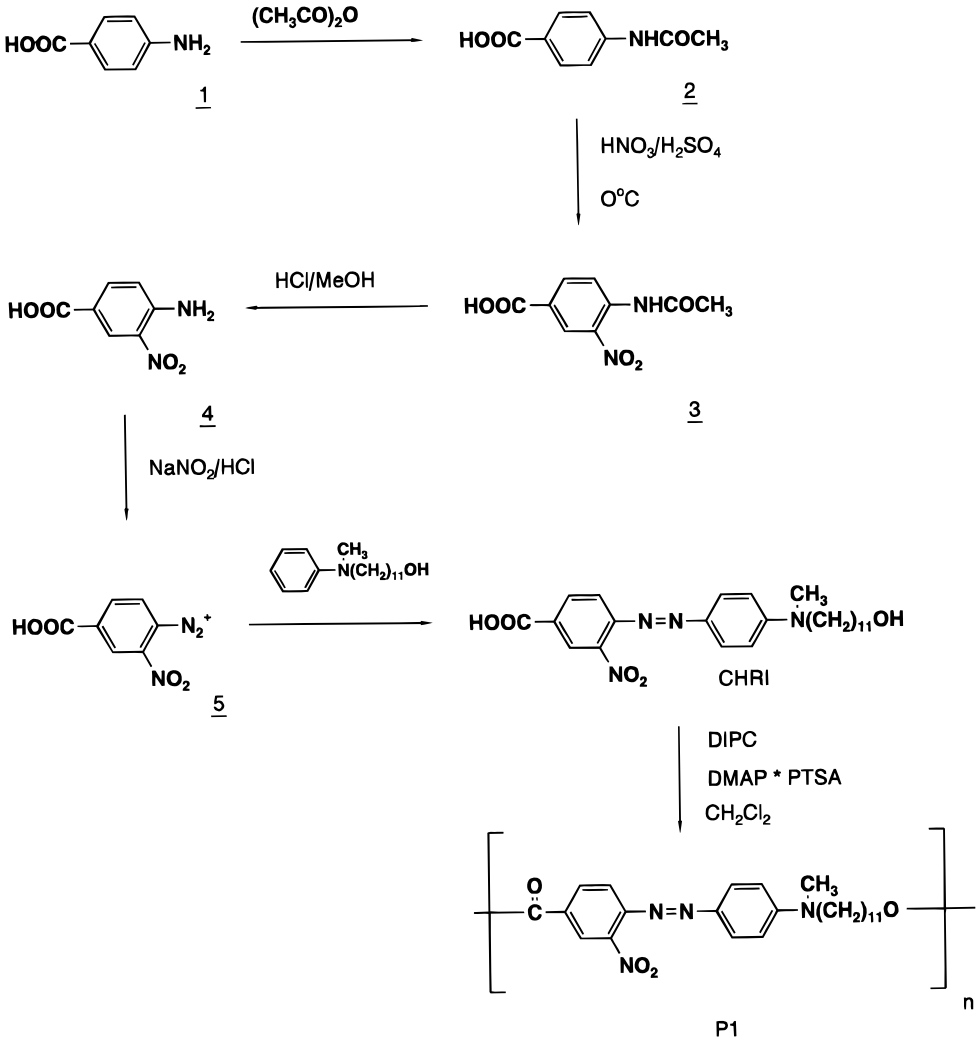

[a] **P1A**−**D** represent a polymer with the same molecular structure but different molecular weights (see Table 1).

6.75 (d, 2H, H3′, H5′), 7.37 (d, 1.08H, H3, H5, 4-HBA), 7.42 (d, 1.01H, H3, H5, 4-HBA), 7.85, 7.87, 7.90 (d, 4H, H2′, H6′, H2, H6), 8.14 (d, 2H, H3, H5), 8.29 (d, 2.0 H, 2H, 6H, 4-HBA). IR (cm^{-1}): 818 (w), 1009 (m), 1049 (s), 1133 (vs), 1159 (m), 1198 (m), 1256 (m), 1380 (m), 1598 (s), 2852 (w, broad); 2923 (w, broad), 3452 (w, broad). Anal. Calcd for ($C_{31}H_{37}O_4N_3$): C, 72.2; H, 7.2; N, 8.6; O, 12.4. Found: C, 72.10; H, 7.2; N, 8.3.

Data for [CHRII$_{0.25}$HBA$_{0.75}$]. ^{1}H-NMR ($CDCl_3$): 1.44 (m, 14H, $(CH_2)^3(CH_2)^9$), 1.69 (m, 2H, $(CH_2)^2$), 1.77 (m, 2H, $(CH_2)^{10}$), 3.09 (s, 3H, NCH_3), 3.53 (t, 2H, NCH_2), 4.34 (t, 2H, $O(CH_2)^{11}$), 6.75 (d, 2H, H3′, H5′), 7.32 (d, 1.44H, H3, H5, 4-HBA), 7.44 (d, 5.11H, H3, H5, 4-HBA), 7.91, 7.93, 7.96 (2d, 4H, H2′, H6′, H2, H6), 8.14 (d, 2H, H3, H5), 8.32 (d, 6.0H, 2H, 6H, 4-HBA). IR (cm^{-1}): 1011 (m), 1051 (vs), 1132 (m), 1160 (vs), 1202 (s), 1259 (s), 1379 (m), 1598 (s), 1740 (s), 2852 (w, broad), 2925 (w, broad), 3450 (w, very broad). Anal. Calcd for ($C_{11.5}H_{11.25}N_{0.75}O_2$): C, 72.0; 5.91; N, 5.5; O, 16.7. Found: C, 71.1; H, 5.6; N, 5.6.

Synthesis

The building block we aimed to synthesize is shown in Figure 2 and consists of an electron donor and electron acceptor connected via a conjugated π-system. To ensure liquid crystallinity, the π-system has to be a rigid, mesogenic unit, consecutive units being connected via a long alkyl chain providing enough flexibility of the whole main chain to be oriented in an electric poling field. The counterbalance of rigidity of the mesogenic unit and flexibility of the alkyl chain determines to a great extent the NLO properties of our material. It is important to stress that the polymer main chain exhibits a head-to-tail arrangement of the dipoles and can therefore only be synthesised via an AB-type of polymerization. The structure of the selected monomer CHRI is shown in Scheme 1.

An azo benzene unit was chosen as the mesogenic unit since it is known that this group is less sensitive to light (cross-linking reactions) than stilbene moieties. To avoid the rather tedious synthesis of a chromophore with the strong electron-withdrawing $-SO_2-$ group[12−14] and to make the synthetic route as simple as possible, a carboxyl group was chosen to function as the electron acceptor and as the reactive group in the polycondensation process. Since the electron-withdrawing effect of the carboxy group is weak, a nitro group was introduced ortho to the azo group to enhance the nonlinear hyperpolarizability of the compound. Unfortunately, both the nitro and the dialkylamino group (compared to alkoxy) reduce the axial to diameter ratio and therefore diminish the mesogenic tendencies of the material.

Scheme 2. Synthesis of *N*-Methyl-*N*-(ω-hydroxyundecyl)aniline (9)

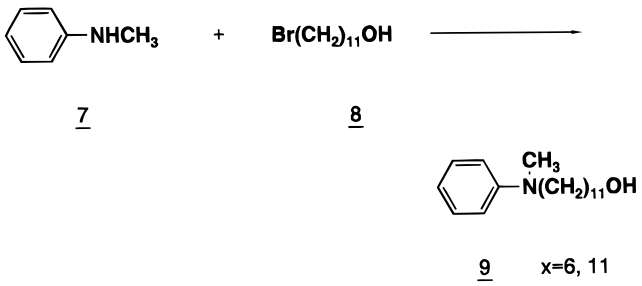

The synthetic route (Scheme 1) comprises the acetylation of *p*-aminobenzoic acid (**1**) followed by nitration of the resulting compound **2** with a mixture of nitric acid/sulfuric acid at 0−5 °C.[28] The protective group is then removed in a methanol/hydrochloric acid mixture to give **4**. After diazotization with sodium nitrite in hydrochloric acid[29] the diazonium salt **5** is coupled with *N*-methyl-*N*-(11-hydroxyundecyl)aniline (**9**) that can be prepared by alkylation of *N*-methylaniline (**7**) with 11-bromoundecanol (**8**) (Scheme 2) giving the monomer CHRI. Alternatively, *p*-aminobenzoic acid (**1**) (Scheme 3) was directly coupled with *N*-methyl-*N*-(11-hydroxyundecyl)aniline (**9**) to give the second type of monomer CHRII. The absence of the bulky nitro group should enhance the probability of obtaining a LC polymer from this monomer (see below).

All monomers CHRI and CHRII were polymerized according to Moore and Stupp[30] via room temperature esterification with dichloromethane as solvent, diisopropylcarbodiimide as condensation agent and (dimethylamino)pyridine/*p*-toluenesulfonic acid as catalyst. See Scheme 1, for the synthesis of the homopolymer of CHRI (polymer **P1**), Scheme 3 for the homopolymer of CHRII (**P2**), and Scheme 4 for the copolymer [$CHRI_{0.5}$-$HBA_{0.5}$] and copolymers [$CHRII_xHBA_{1-x}$], $x = 0.25, 0.5, 0.75$. The monomers are all nearly insoluble in dichloromethane but go into solution shortly after addition of diisopropylcarbodiimide. Solvents like dimethylformamide or dimethylacetamide, which are better solvents for the monomers, only led to low molecular weight samples. The polymers were usually precipitated from methanol. Reprecipitation from dichloromethane/methanol or chloroform/methanol worked for none of the compounds since colloidal solutions were formed (the polymers precipitate from strongly acidified methanolic solutions; however, the higher content of H^+ ions leads to higher conductivities of the spin-coated films and should therefore be avoided). Sufficient purification can be obtained by Soxhlet-extraction with acetone or ethyl acetate for 1-2 days. Further polycondensations (of monomer CHRI) were carried out according to Higashi's method of direct polycondensation with diphenyl chlorophosphate as condensation agent, pyridine as solvent, and a reaction temperature of 120 °C[31] (see below).

Scheme 3. Synthesis of 4-Carboxy-4′-[*N*-(11-hydroxyundecyl)-*N*-methylamino]azobenzene (CHRII) and Polymer P2

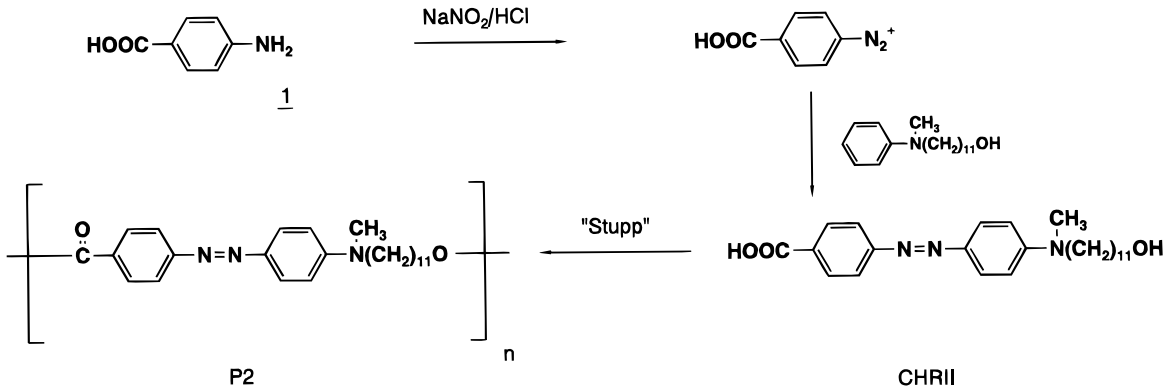

Scheme 4. Synthesis of the copolymers [$CHRI_{0.5}HBA_{0.5}$] and [$CHRII_xHBA_{1-x}$] from *p*-Hydroxybenzoic Acid (HBA) and Monomers CHRI and CHRII, Respectively

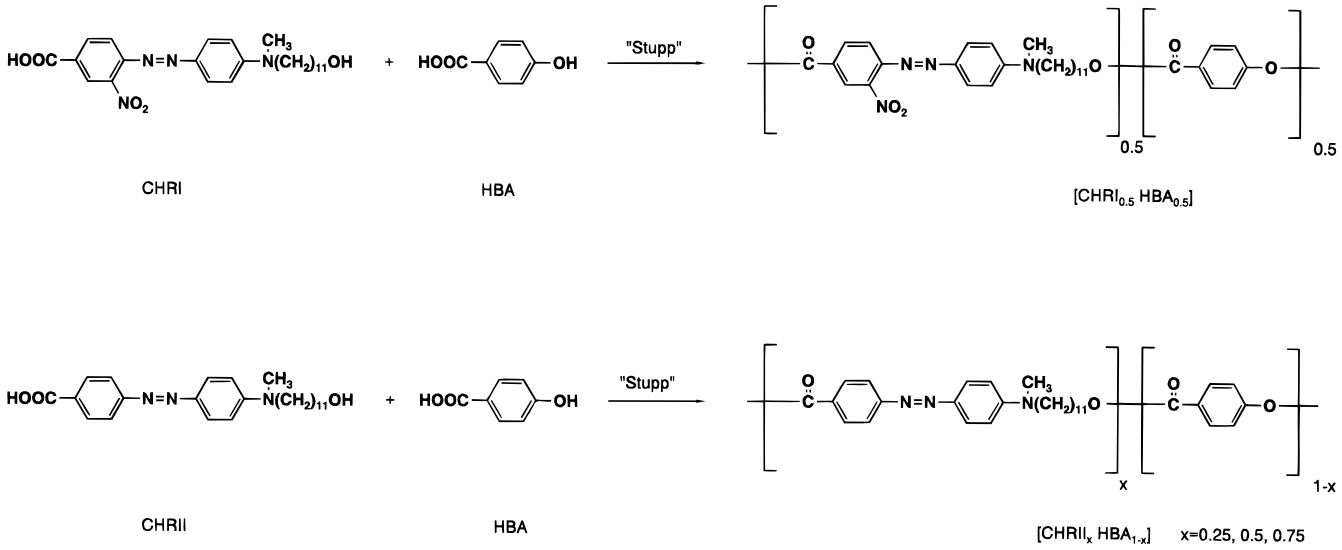

Table 1. Molecular Weight Data of P1A−D (Homopolymers with CHRI), P2 (Homopolymers with CHRII), and Copolymers of Chromophores and HBA, [$CHRI_{0.5}HBA_{0.5}$] and [$CHRII_xHBA_{1-x}$] Measured by GPC with Polystyrene as Standard[a]

polymer	M_p	M_w	M_n	PD	DP_p	method
P1A	≈1 500	≈1 500	≈300	≈5−6	2−3	Stupp,[30] DMF
P1B	5 477	5 106	1 224	4.17	12	Higashi[31]
P1C	29 908	30 173	7 860	3.84	66	Stupp,[30] CH_2Cl_2
P1D	39 478	40 129	11 172	3.59	87	Stupp, CH_2Cl_2, PTSA·DMAP complex[30]
P2						see **P1D**
[$CHRI_{0.5}HBA_{0.5}$]	43 736	45 750	17 349	2.64	160	see **P1D**
[$CHRII_{0.75}HBA_{0.25}$]	57 207	56 089	13 794	4.07	167	see **P1D**
[$CHRII_{0.5}HBA_{0.5}$]	36 803	38 129	11 052	3.45	145	see **P1D**
[$CHRII_{0.25}HBA_{0.75}$]						see **P1D**

[a] M_p = peak molecular weight, M_n = number average molecular weight, PD = polydispersity (M_w/M_n), DP_w = degree of polymerization with respect to M_w. In calculating DP_w for the copolymers, M_w/M(repeating unit), the relative ratio of CHRI and CHRII, respectively, and HBA was taken into account. PTSA is *p*-toluenesulfonic acid and DMAP is (dimethylamino)pyridine. Methods: for variation in the synthesis method used, see text. Samples **P2** and [$CHRII_{0.25}HBA_{0.75}$] were not further analyzed since they were not used for NLO measurements.

To further improve the LC behavior of the polymers, copolymers of the monomers CHRI and CHRII with hydroxybenzoic acid (HBA) were prepared (Scheme 4). Since the reactivity (copolymerization parameters) of CHRI/CHRII and HBA are probably different, two methods were tested in order to obtain random copolymers. These make for good processibility of the materials. In the first method, over 8 hs, monomers CHRI and CHRII, respectively, HBA, and a minimum amount of diisopropylcarbodiimide were added in small batches to the reaction mixture. Only the last batch contained a larger excess of diisopropylcarbodiimide. In the second method, all compounds were combined and stirred at room temperature for 3 days. The properties of the resulting polymers were very similar. This might be attributed to the very low solubility of HBA in dichloromethane which reduces the accessibility of HBA during the polycondensation process and impedes the uptake of HBA into the polymer chain. The higher reactivity of HBA (two aromatic functional groups) is obviously compensated by the lower solubility of HBA in dichloromethane.

The various polymers and their properties are summarized in Table 1, which is also helpful as a summary of the nomenclature.

Characterization of the Polymers. GPC was carried out on all polymers using chloroform as a solvent. For **P1D** a bimodal distribution emerged, characterized by a distinct shoulder at around 8 min elution time. The molecular weight data determined from the elution curves are collected in Table 1 together with the various methods used to prepare the polymers. As already mentioned, dimethylformamide was used as solvent in Stupp's room temperature esterification. In agreement with Stupp's own results,[30] only low molecular weight products were produced. Oligomeric species were obtained with Higashi's method[31] of direct polycondensation with diphenyl chlorophosphate as condensation agent, pyridine as solvent, and a reaction temperature of 120 °C. The production of only oligomeric species can be attributed to the fact that Higashi's method works very well with aromatic functional groups but is less efficient for alkyl hydroxyl or carboxyl groups. When dimethylformamide is substituted by dichloromethane (Stupp's method), the molecular weight of the polymer formed is considerably enhanced. In contrast to the monomer, the polymer is readily soluble in dichloromethane, which makes it possible to perform the polyesterification in this solvent. The molecular weight is further increased by adding the catalysts (dimethylamino)pyridine (DMAP) and *p*-toluenesulfonic acid (PTSA) as a preformed complex so that the reaction can be carried out anhydrously with a fixed 1:1 ratio of the two compounds. The peak molecular weight M_p is now around 40 000, corresponding to a degree of polymerization DP_w of 87.

Table 1 shows that the polydispersity decreases with increasing molecular weight, but even for the highest molecular weight sample the polydispersity index (DP_w = 3.8) is considerably above the theoretical value of 2.0. However, it should be mentioned that a molecular weight of M_w = 40 000 is one of the highest published so far for NLO-active main chain polymers of this type.

The ^{1}H-NMR spectra of monomer CHRI and of polymer **P1B** were taken. The polymer spectrum, when compared with that of the monomer, clearly demonstrates the presence of a small fraction, around 5-10%, of free CH_2OH end groups. The relative intensities (integrals) of the two peaks at ca. 3.5 ppm lead to an evaluation of $DP_n \cong 10$ (degree of polymerization with respect to the number average molecular weight), giving a M_n of about 4600. The discrepancy between this estimation and the one given in Table 1 (DP_n = 2.7 and M_n = 1224) suggests that the molecular weights in Table 1 should only be understood as lower estimates.

The spectrum of **P1C** is very clear, revealing no detectable concentration of end groups. It thus corroborates the high molecular weight of this material. However, it should be stressed that the GPC was calibrated against polystyrene standards, a polymer with a completely different molecular shape compared to our main chain systems. Thus the evaluation of M_n from the integrals of the two overlapping peaks in the spectrum of **P1B** is not unambiguous.

Studies with the polarizing microscope showed that monomer CHRI melts into an isotropic liquid. As already mentioned above, this might be due to the bulky nitro group, which reduces the axial to diameter ratio and therefore the probability of the existence of an LC phase. All polymers **P1A−D** formed from CHRI gave an isotropic melt.

Thermogravimetric analysis was also carried out. For instance **P1D** was shown to be stable up to 280 °C under a nitrogen atmosphere, giving a sufficient temperature window for NLO measurements even at elevated temperatures. Further, the polymers were analyzed by DSC. In **P1D** a broad endothermic peak was observed at around 112 °C with a ΔH of 26.9 J/g (heating rate: 20 K/min). This peak is only observed in the first heating curve and is not displayed in any other of the heating or cooling experiments. Within the investigated temperature region no indication of a liquid crystalline

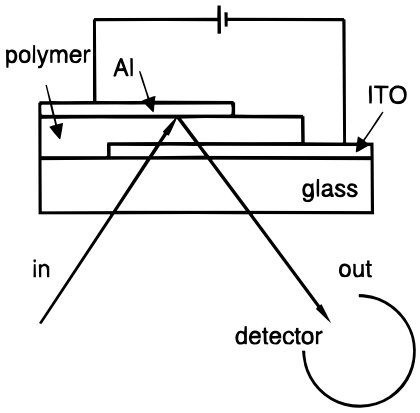

Figure 4. Sample geometry and schematic setup for the linear Pockels experiment in reflection.

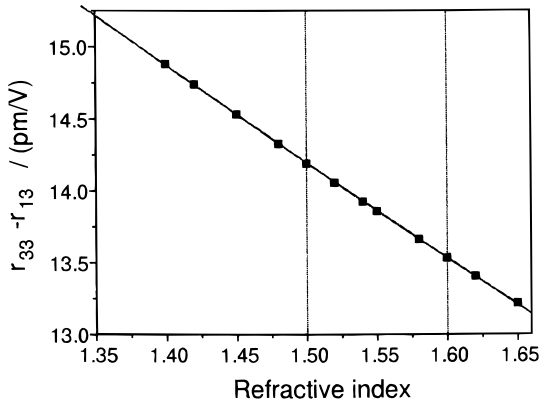

Figure 5. Difference of the electrooptical coefficients $r_{33} - r_{13}$, as calculated from the analysis leading to eq 2, as a function of refractive index with $\lambda = 632$ nm, $\delta I = 300$ μV, $I_m = 1$ V, $\Omega = 45°$, $f = 1$, and $U = 10$ V. Most of the refractive indices of chromophore-substituted polymers of the type investigated can be found in the region indicated by the vertical lines in the diagram.

phase transition can be found. This is in agreement with studies carried out with the polarizing microscope demonstrating that **P1D** is, after melting, an amorphous nonbirefringent material. Higher resolution DSC measurements reveal a glass temperature at 54 °C.

X ray studies were performed to investigate the melting peak being only in the first heating cycle. At room temperature the polymer is a semicrystalline material, as indicated by a structured pattern of the peak in the wide angle region. The pattern is not changed at 70 °C. At 150 °C, well above the melting temperature, only an amorphous halo is displayed. When cooled to room temperature (cooling rate: 10 K/min) the crystallinity is not recovered. A peak with a rather low intensity in the small angle region at $2\vartheta = 5°$ can be assigned to the length of the mesogenic unit (≈13 Å). This peak can already be found in the diffractograms at 70 and 30 °C as a shoulder at around $2\vartheta = 5°$.

Characterization of the NLO Properties. (a) Linear Pockels Method. The NLO measurements were performed with a linear Pockels setup, first proposed by Teng and Man,[32] van der Voorst and van Weerdenburg,[33] and Röhl, Andress, and Nordmann,[34] where phase change is converted to intensity variation: the electrooptical effect of the material alters the birefringence, leading to a rotation of the plane of polarization of the linearly polarized light. Since polarizer (in front of the sample) and analyzer (behind) are crossed, this phase shift is transformed into a change in intensity behind the analyzer.

Although straightforward in principle, there are many possible complications in this technique. Levy *et al.*[2,35] discuss multiple reflections within the multilayer structure of the sample and the component of absorption that can be modulated by the Pockels field. We shall in this paper limit ourselves to preliminary NLO measurements, returning in a later paper to precise quantitative measurements and to the points of principle and details of theory raised by Levy *et al*. Already with measurements of modest accuracy (10%), one can examine the three points of principle we wish to establish: that nematic MC polymers show a huge enhancement over their nonnematic analogues, response is high-polymer like involving whole chain motions, and that the stability of the glassy state is very great.

We perform our experiments in reflection (at 45°) rather than in transmission[33] and obtain the difference $r_{33} - r_{13}$ in the electrooptical coefficients. Figure 4 shows a cell and how, in reflection, light is passed through the sample.

The dc poling field E_{pol} and the ac (700 Hz) modulating (Pockels) field E_{ac} are applied on the same electrodes. A light beam is set to an optimal operating intensity,[33] I_{op}, and the modulated intensity δI resulting from the refractive index variation created by E_{ac} is detected with high accuracy by a lock-in amplifier. Because measurements can be made quickly, we can observe δI changing as a function of time after E_{pol} has been switched on or off; that is, we can measure the buildup or decay of $\chi^{(2)}$ as chains respond to establish or relax noncentrosymmetric order (the poled state).

In isotropic polymers we can reasonably assume that $r_{13} = r_{33}/3$. In nematic polymers r_{13} is much reduced by the high orientational order. We have no separate measurements of r_{13} and hence can only estimate $\chi^{(2)}_{333}$.

Using the refractive index $n = 1.55$ (and neglecting anisotropy in this analysis[33]), $\lambda = 632.8$ nm, and U (the modulating voltage) in volts, one obtains

$$r_{33} - r_{13} = 1.15\frac{\delta I}{I_{op}U}10^5 \text{ (pm/V)} \qquad (2)$$

for the electrooptical (EO) coefficient difference. The EO coefficients are related to $\chi^{(2)}$ by $\chi^{(2)}_{333} = -n_e^4 r_{33}/2$ and $\chi^{(2)}_{113} = -n_o^4 r_{13}/2$ where n_e and n_o are the extraordinary and ordinary refractive indices. For the calculation of values in this paper, it was assumed that both are equal to 1.55. By putting a range of values for the refractive index into the analysis leading to eq 2, one obtains a spread of possible values for $r_{33} - r_{13}$. Figure 5 shows the outcome and hence the uncertainty in the EO coefficients resulting from uncertainty in the refractive index.

Some of the concerns about EO measurements can be addressed in a general manner. Multiple reflections have been accommodated by the use of a reflection factor f. We have assumed naively $f = 2$, since the rear face is silvered and the front face is transparent (ITO and glass). It has been argued[33] that for these electrodes and for our sample thicknesses this is a reasonable assumption. The danger is that, in a Fabre−Perot cell of high finesse, the light would take many passes

through the optically nonlinear medium and one would thereby overestimate $\chi^{(2)}$, having underestimated the optical path length using $f = 2$. We have calculated the effective finesse of our sample assembly and find that it is indeed low, reassuring us that $f = 2$ is realistic. To check this, we need to perform reflectivity measurements as a function of incident angle. Levy *et al.*[35] show that reflectivity and modulated absorption both induce an error, a measure of which is the modulated response at the two optimal operating points being no longer the same size. We find a 10% difference in the modulated signals that gives us confidence that the error induced by these effects is not major. (We thank Mr. A Koch for checking this experimentally.)

In time-resolved measurements we necessarily have both static and modulating fields, E_{pol} and E_{ac}. One could argue that, especially when E_{pol} and E_{ac} are of similar magnitude, $\chi^{(3)}$ effects might be present at the modulating frequency due to the additional presence of E_{pol}. We have in effect tested for this and found the effect absent. The poled nematic polymers exhibiting the large $\chi^{(2)}$ responses can be quenched with E_{pol} applied and then $\chi^{(2)}$ remeasured with $E_{pol} = 0$ where $\chi^{(3)}$ effects are necessarily absent at the modulating frequency. The results are identical.

Equally, one could suspect that the large effects seen in nematic polymers are due to birefringence created by E_{ac} inducing more orientational order. The time-resolved experiments we shall present suggest otherwise—the order is polar and takes minutes to induce, rather than responding at the 700 Hz of E_{ac}. In any event, the *equally* large response in the quenched state appears to rule out this explanation. The tandem effect of E_{pol} and E_{ac} in modulating birefringence can also be ruled out by these arguments.

(b) Isotropic Polymers. All films prepared from **P1D** showed a spontaneous polarization (before poling) with EO coefficients in the range $r_{33} - r_{13} = 0.12 - 0.21$ pm/V ($\delta I/I_{op} = (16-28) \times 10^{-6}$, $U = 15$ V). This might be attributed to surface effects. The values arising are very small compared with the values of interest in the nematic polymers below.

Depending on the individual sample, the coefficients $r_{33} - r_{13}$ after poling at 85 °C with a field of the order of 20 V/μm and a cooling rate of 0.2 K/min, were between 0.75 and 1.56 pm/V ($\delta I/I_{op} = (65-136) \times 10^{-6}$, $U = 10$ V). Assuming an isotropic model (amorphous polymer before poling, therefore with $3r_{13} = r_{33}$) one obtains

$$r_{33} = |1.1 - 2.3| \text{ pm/V}$$
$$r_{13} = |0.38 - 0.78| \text{ pm/V} \quad (3)$$

or converting to $\chi^{(2)}$

$$\chi^{(2)}_{333} = \frac{-n_e^4 r_{33}}{2} = 3.1-6.7 \text{ pm/V}$$
$$\chi^{(2)}_{113} = \frac{-n_o^4 r_{13}}{2} = 1.1-2.2 \text{ pm/V} \quad (4)$$

with $n_e \cong n_o \cong n = 1.55$.

(c) Dynamics of Poling. Normalized time-resolved electrooptical measurements are depicted in Figure 6.

As expected, relaxation occurs very quickly when a temperature close to T_g is reached. Therefore, relaxation data for $T > T_g - 10$ were not accessible. These

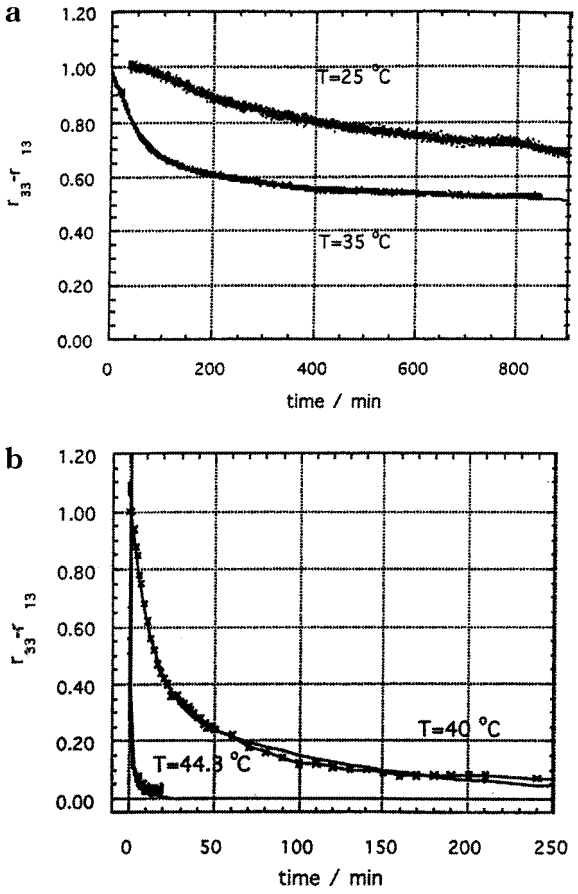

Figure 6. Normalized relaxation curves of **P1D** at various temperatures.

Table 2. Relaxation Times τ_i for P1D at Different Temperatures[a]

temp/°C	τ_1/min	τ_2/min
25	350(2)	7280(102)
35	62.6(3)	4860(47)
40	12.3(6)	116(7)
44.3	0.43(1)	5.4(3)

[a] The values in brackets are the errors of the respective digit derived from the fit of eq 5 to the relaxation curves in Figure 6.

curves characteristically show a very steep decrease of the electrooptical signal directly after the poling field has been switched off (see below). The relaxation curves were fitted to

$$\chi^{(2)}(t) \cong \sum_{i=1}^{n} A_i e^{-t/\tau_i} \quad (5)$$

to yield the relaxation times τ_i (Table 2).

The τ_i from the first and second relaxation are used to construct an Arrhenius-type diagram (Figure 7). The large slope of the straight lines indicates a strong temperature dependence. Equation 6

$$\tau(T) = \tau_0 e^{E_a/kT} \quad (6)$$

was used to determine the activation energies E_a of the relaxation processes, giving a value of 250(71) kJ/mol for the first and 263(97) kJ/mol for the second relaxation. It should be noted that this division into two relaxation processes is purely formal. An assignment to certain molecular processes (e.g., small angle mobility

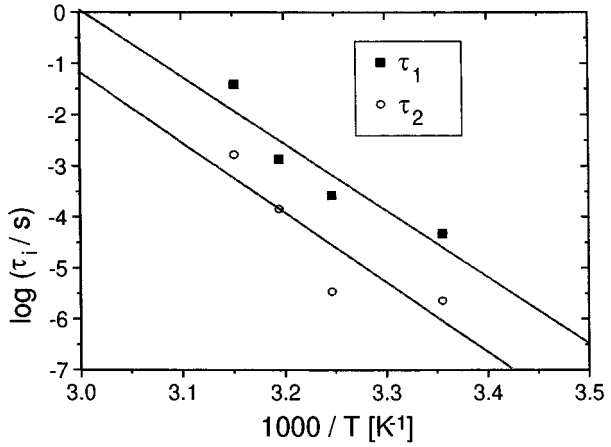

Figure 7. Relaxation times τ_i determined from Figure 6 in an Arrhenius-type plot for the evaluation of the activation energy E_a in eq 6.

of the chromophore in contrast to a rotation/mobility of the matrix on a larger scale) is deliberately avoided here. Moreover, the construction of straight fit-lines in Figure 7 is only possible since the temperature interval is very small.

(d) Nematic Polymers. Phase Behavior. As discussed in the Introduction, liquid crystallinity is absolutely necessary for achieving the desired improvement of the NLO properties. It was therefore necessary to modify the structure of polymer **P1** so that a new polymer would exhibit liquid crystallinity. The first attempt was to remove the bulky nitro group (Scheme 3) in order to enhance the axial to diameter ratio of the mesogenic unit. Although the synthesis is facilitated, the hyperpolarizability of the resulting chromophore can be expected to be considerably smaller than that of monomer CHRI. When studied with the polarizing microscope, monomer CHRII melted into a liquid crystalline melt in contrast to monomer CHRI, which gave only an isotropic melt. However, when polymerized, polymer **P2** only showed an LC phase when sheared. This LC phase is "stable": even when heated above the isotropization temperature, the LC phase is reobtained after cooling without any further shearing.

The structure of the polymer is evidently not yet optimal for the formation of an LC phase: either the mesogenic unit is too short (or insufficiently rigid) or the alkyl chain is too short (insufficient flexibility, the mesogenic units are not separated "enough" and therefore cannot organize themselves sufficiently to form an LC phase). We decided to test the first assumption by copolymerizing the monomers CHRI and CHRII, respectively, with *p*-hydroxybenzoic acid HBA, which extends the length of the mesogenic unit by one aromatic ring (Scheme 4). The amount of HBA built into the main chain was checked with ^{1}H-NMR spectroscopy and was in perfect agreement with the feed ratio. All polymers are easily soluble in tetrahydrofuran, chloroform, or 1,1,2,2-tetrachloroethane. Usually, dissolution of the polymers in these solvents led to slightly cloudy solutions. These small amounts of insoluble polymer might possibly be attributed to the portion of polymer with a higher content of HBA blocks in the polymer chain (note that already pentamers of HBA are nearly insoluble in all organic solvents). The insoluble fraction increased with increasing HBA/CHRII ratio. All copolymers with various CHRII/HBA ratios and even the 50/50 copolymer of CHRI/HBA exhibit a nematic LC phase. Phase transition temperatures are given in Table 3. The temperature for the transition $n \leftrightarrow i$ rises with increasing HBA content in the main chain. The phase transitions n ↔ i were rather broad. The advantage of this copolymerization is obvious: the properties of the resulting polymer, e.g., the phase transition temperature, the glass transition temperature, solubility, or the quality of the polymer films can be tailored by changing the HBA/CHRII ratio.

Table 3. Phase Transition Temperatures from the Liquid Crystalline State into the Isotropic Melt and Vice Versa for P2 and the CHR/HBA Copolymers[a]

polymer	T/°C, LC → i	T/°C, i → LC
P2	only LC when sheared	
[$CHRI_{0.5}HBA_{0.5}$]	155−160	150−140
[$CHRII_{0.75}HBA_{0.25}$]	135−145	130−124
[$CHRII_{0.5}HBA_{0.5}$]	210−220	190−175
[$CHRII_{0.25}HBA_{0.75}$]	>240, decomposition	

[a] The phase transitions were rather broad. The first temperature is the onset, the second, the end of the phase transition. Heating/cooling rate: 20 K/min.

Unfortunately, spin-coated films of polymers [$CHRII_xHBA_{1-x}$], x = 0.25, 0.5, 0.75, and [$CHRI_{0.5}HBA_{0.5}$] were completely isotropic. This can be explained by the large centrifugal forces acting on the molecules during the spin-coating process in combination with a very fast evaporation of the solvent. However, polymer [$CHRII_{0.5}HBA_{0.5}$] can be transferred into the LC state by tempering the film at 65−80 °C for 5 min. The transition of the film from the isotropic into the LC state was observed by polarized microscopy. The film should not be heated above 100 °C since the film collapsed and small polymer droplets were formed on the surface. The tempering has to be done prior to the evaporation of the top electrode. When tempered after the evaporation of aluminum, the reorganization of the main chains in the film leads to strong internal mechanical forces which finally break and destroy the electrode. Tempering the films of polymer [$CHRII_{0.25}HBA_{0.75}$] did not induce liquid crystallinity. Only when cast from solution was an LC film obtained. The nitro copolymer [$CHRI_{0.50}HBA_{0.50}$] was liquid crystalline when cooled in the melt but not used for NLO measurements.

Since the tempering process was the easiest to perform, further data were only collected from the polymer [$CHRII_{0.50}HBA_{0.50}$]. The physical data are as follows. The TGA indicates a thermal stability up to 230 °C (under nitrogen). The DSC diagram revealed a broad endothermic peak between 42 and 65 °C (possibly melting of the crystalline portion of the polymer) and a T_g of 65 °C (only displayed in the heating cycle after rapid cooling from 230 to 25 °C to prevent any recrystallization). The GPC measurements gave a molecular weight of around 38 000 with a polydispersity of 3.5. The pattern of the X-ray diffractogram is very similar to that of **P1**.

(e) Nematic Polymers. NLO Response. Figure 8 shows the poling (t = 0 min) and depoling (t = 10 min) behavior of polymer [$CHRII_{0.50}HBA_{0.50}$] with an applied ac voltage of 7 V and a dc voltage of 10 V at 90 °C (film thickness: ca. 0.2−0.4 μm) in the LC state.

To illustrate the different magnitude of the NLO response, data obtained from a film of **P1D** with both an ac and dc voltage of 10 V at 35 °C are shown as well.

Comparing the two data sets, four features of the poling behavior of polymer [$CHRII_{0.50}HBA_{0.50}$] are completely different from polymer **P1**:

(1) The absolute value of the NLO signal [$\delta/I_{op} \propto (r_{33} - r_{13})$ see eq 2] is higher by a factor of approximately 10 (typical values of $\delta I/I_{op}$ up to 1.3 × 10^{-3} were

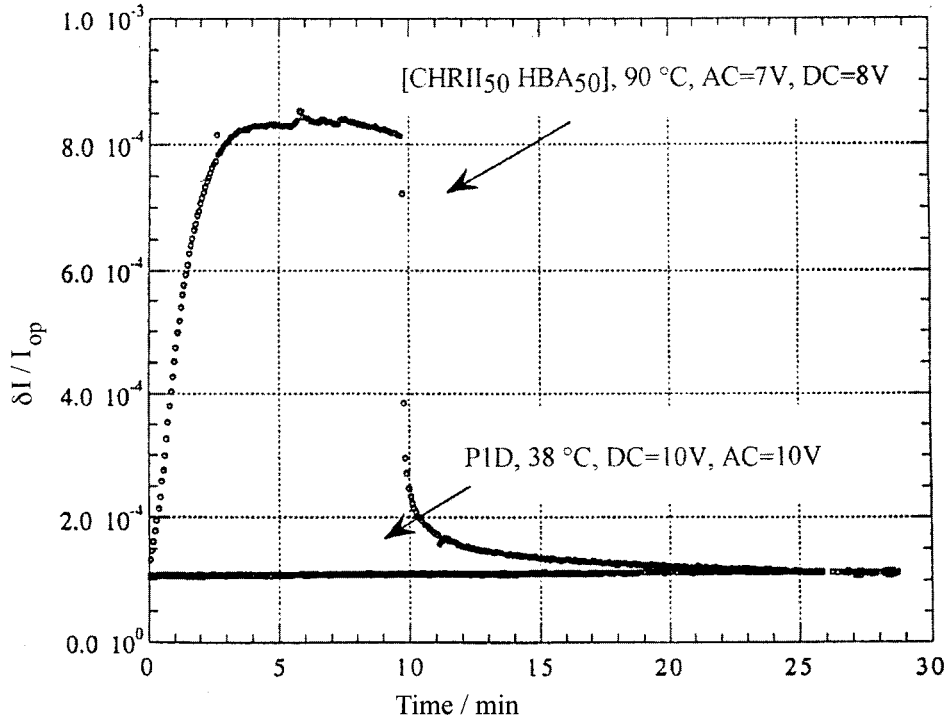

Figure 8. Comparison of the poling and depoling behavior of [$CHR_{50}HBA_{50}$] and **P1D** at 90 °C and 38 °C, respectively. The poling conditions are given in the diagram.

measured for other films at room temperature with dc = 0 V, ac = 7 V). Note that the measuring (ac) field is smaller in the case of polymer [$CHRII_{0.50}HBA_{0.50}$]. These values are "surprisingly" high since (I) now only 77% (by weight and hence approximately also by volume) of the chain contains chromophores rather than 100% as in P1 chromophores were substituted by HBA, a molecule with a very small hyperpolarizability) and (II) the hyperpolarizability of the chromophore CHRII can be expected to be considerably lower than that of CHRI (parameter β_{333} in the tensor version of eq 1). If polymer [$CHRII_{0.50}HBA_{0.50}$] were an amorphous system, one would expect (same poling conditions assumed) a decrease of $r_{33} - r_{13}$ compared to the case of **P1**. Instead, one observes a large increase in the NLO response. This can only be explained by the different phase behavior of the LC polymer [$CHRII_{0.50}HBA_{0.50}$].

(2) The poling of polymer **P1** is nearly instantaneous above T_g, the NLO response jumping to higher values within a second or so presumably due to small angle reorientation of the chromophore (and possibly smaller $\chi^{(3)}$ contributions). By contrast, polymer [$CHRII_{0.50}HBA_{0.50}$] can only be poled within acceptable time limits at a temperature considerably above $T_g = 65$ °C, in this case 90 °C. It shows a pronounced, high polymer-like dynamics and reaches a plateau after approximately 5 min. This was observed for all films. It also suffers the jump of **P1**, but relative to its large, slow response, this is a small effect. Both the differences in magnitudes and in the dynamics suggest very different response mechanisms: in **P1** there is a local rearrangement of chromophores to give a dipolar bias. In the LC copolymers entire chain motion is apparently involved in biasing larger numbers of chromophores. Only in the LC phase does the electric field act on the cooperative (effective) dipole moment of the whole main chain, therefore inducing a larger polar bias in comparison with the amorphous polymer **P1**.

(3) Depoling suggests the same conclusions. Polymers **P1** exhibit classical glassy behavior where, although gross motion of chains becomes frozen out, local motion of segments is still possible and dipolar order can be relaxed away. Polymer **P1** relaxed so quickly, even at $T_g - 10$ °C, that the measurement of the relaxation process could not be followed with the experimental setup. When the electric field was switched off at room temperature, deep in the glassy state, the films of polymer **P1** often lost half of their NLO response. This is not unusual or unexpected for a polymeric glass. For nematic copolymers in the LC glassy state, chains are equally unable to move in a gross sense. Since their dipolar order arose from gross rearrangements of the main chains, it is thereby largely preserved on glassification. Up to 10% of the response was lost rapidly; thereafter the films were apparently indefinitely stable. We emphasize that the films are rapidly cooled to a glassy rather than semicrystalline phase. For the copolymers, the glassy state is LC; for **P1** it is isotropic.

(4) We can rule out the origin of our observations being $\chi^{(3)}$ contributions (involving the applied dc field). Such contributions are independent of the extent of polar order induced, requiring only the order of quadrupolar symmetry. Loss of EO activity after the removal of the poling field while preserving nematic character is only compatible with dipolar order and its subsequent loss. Also ruling out $\chi^{(3)}$ as the origin of our effects is the failure of the EO signal to vanish *instantly* when the dc field is removed.

Applying eq 2 to estimate the difference of the electrooptical coefficients $r_{33} - r_{13}$, one obtains, depending upon the particular sample and with the modulating voltage $U = 7$ V (see Figure 8):

$$\frac{\delta I}{I_{op}}([CHRII_{0.50}HBA_{0.50}]) \cong (0.85-1.3) \times 10^{-3} \Rightarrow r_{33} - r_{13} = 14-21 \text{ pm/V}$$

$$\Rightarrow \Delta\chi^{(2)} = 40-61 \text{ pm/V}$$

Since the r_{33}/r_{13} ratio is not known in the case of the highly anisotropic polymer [$CHRII_{0.50}HBA_{0.50}$], $\chi^{(2)}$ values cannot be calculated from the values given above. (The connection with $\chi^{(2)} \approx 0.5rn^4 \cong 2.5r$ is explained in the text.)

Conclusions

Theoretical considerations published in the literature implied that liquid crystalline semiflexible main chain polymers with a head-to-tail structure should give rise to a giant dipole moment. This large effective dipole moment of the main chain is built up from the individual monomeric units. The number of these units "interacting" together depends on the particular structure of the polymer, the temperature, the electric poling field, and the energy of the hairpins where the polymer chain changes its direction. In this paper, we reported on the synthesis and characterization of semiflexible polyesters containing an NLO-active azo chromophore as the basic building block. Sufficient flexibility along the main chain is guaranteed by linking the azo chromophore together via a long alkyl spacer (CHRI, Scheme 1). With Stupp's method of direct polycondensation, polymer samples with a molecular weight of 40 000, a polydispersity index of 3.6, and a glass transition temperature T_g of 54 °C were obtained. However, DSC and X-ray measurements as well as studies with the polarizing microscope revealed that the polymers were not liquid crystalline. Accordingly, the NLO coefficients were relatively low (the difference $r_{33} - r_{13} = 0.75-1.3$ pm/V) and in the range typical for amorphous polymers.

By copolymerizing a similar azo chromophore CHRII with various amounts of *p*-hydroxybenzoic acid (HBA), copolyesters could be synthesized that exhibit a (presumably nematic) liquid crystalline phase. The phase transition temperatures depend on the HBA/CHRII ratio. The copolymers were readily soluble in organic solvents. However, when spin coated from solution, optically clear but isotropic films were obtained. In the case of the 50/50 copolymer of CHRII and HBA, the films could be transferred into the liquid crystalline state by tempering at elevated temperature. This polymer with a molecular weight of 38 000 (and hence a DP $\sim$ 72), a polydispersity of 3.5, a glass transition temperature of 65 °C, and a LC $\leftrightarrow$ i temperature of 210−220 °C was selected to investigate the NLO behavior. Despite the smaller hyperpolarizability of CHRII compared to CHRI and a smaller concentration (77%) of CHRII in the polymer chain, considerably higher electrooptical coefficients $r_{33} - r_{13}$ of up to 21 pm/V (depending on the individual sample, an increase by a factor between $\times$10 and $\times$20) were obtained. The nature and concentration of the chromophores might have otherwise suggested a reduction in $r_{33} - r_{13}$ of $\times$2 or more. We conclude that the effective enhancement of between $\times$20 and $\times$40 or more over the NLO response of the isotropic analogue is due to the collective response of the hairpinned PLC. The corresponding $\chi^{(2)}$ values are in the range 40−62 pm/V.

The performance of our NLO polymers can be compared with that of optimized side chain NLO polymers. Miller[2] discusses a wide range of such polymers, for instance those of Singer *et al.*[7] with polyacrylate backbones and pendant chromophores of great potency—conjugated phenyl-azo groups with $=C(CN)_2$ acceptors. r_{33} values of 18 pm/V are reported at $\lambda = 799$ nm. Still longer phenyl-azo conjugated groups with the same acceptor[39] give $r_{33} \approx 27$ pm/V (at $\lambda = 633$ nm). These are comparable to d_{33} values measured by SHG (keeping in mind differing poling fields) in analogous polymers discussed by Gonin *et al.*[2] and are considered among the best available. Ours are comparable, but one must recall that our poling fields are factors of 10 smaller and our chromophores very much weaker. Thus with higher poling fields, higher chromophore β values, and longer chains we expect $\chi^{(2)}$ values very many times this figure. (With light of $\lambda \sim 632$ nm, there is some resonance enhancement of the β value which gives a higher $\chi^{(2)}$. Measurements should ideally be at $\lambda \sim 1.2$ μm. However, the enhancement of $\chi^{(2)}$ for reasons of molecular organization (putatively hairpins) on going from **P1** to CHRII/HBA is not related to this observation about resonance. Nor are the further enhancements due to increasing chain length and poling field affected by this concern.)

The relaxation of the nonlinear optical response was drastically reduced. Below T_g no perceptible decline in $\chi^{(2)}$ could be seen in several months. Although very similar in structure, the NLO properties of the amorphous and liquid crystalline polymer were completely different. The large NLO coefficients of the liquid crystalline polymer, the characteristic high polymer time scales and dynamics of the buildup of the poled state, and the long temporal stability are all clear evidence for our theoretical model that a large effective dipole moment is built up from the individual repeating units along the chain of a head-to-tail semiflexible main chain polymer. In accordance with the theory, this effect only occurs in liquid crystalline polymers and not in the related but nonnematic polymers. However, a more thorough theoretical analysis is not possible yet since details of the role played by chain conformations are revealed only by studying the temperature and field dependence of the plateau value of $\chi^{(2)}$. Further investigations are therefore necessary to establish a more detailed picture of NLO-active liquid crystalline semiflexible head-to-tail main chain polymers. The results of these studies will be published in a forthcoming publication. We shall also address the problems[35] associated with quantitatively accurate measurements of $\chi^{(2)}$ by the linear Pockels method.

Acknowledgment. We acknowledge with gratitude the help of Dr. F. Wittmann who wrote the controlling program for the experimental setup, Dr. H. Hirschmann for some experimental advice, Dr. S. Moratti and Dr. J. Steinke for critical discussions about the synthesis of the copolymers, Dr. S. Butler for the GPC measurements, Dr. C. He for the X-ray data and the EPSRC for financial support for C.H. in the period 5.94−6.95 when the work was carried out. We are grateful to Dr. Moratti for continuing to give us critical advice during the interpretation of the NLO results and the writing of this paper.

Supporting Information Available: Figures including the ^{1}H-NMR spectrum of CHRI, the ^{1}H-NMR spectrum of **P1B**, the ^{1}H-NMR spectrum of **P1C** (the assignment of the peaks being given in the experimental part), and thermogravimetric analysis, X-ray scattering, GPC, and DSC of **P1D** (9 pages). Ordering and Internet accessing instructions are given on any current masthead page.

References and Notes

(1) Möhlmann, G.R. In *Nonlinear Optics: Fundamentals, Materials and Devices*; Miyata, S., Ed.; North Holland: Amsterdam, 1991; p 415.

(2) *Organic Thin Films for Waveguiding Nonlinear Optics*; Kajzar, F., Swalen, J. D., Eds.; Vol. 3 of Advances in Nonlinear Optics; Gordon and Breach: Amsterdam, 1996.
(3) Möhlmann, R.; Horsthuis, W. H. G.; van der Vorst, C. P. J. M.; McDonach, A.; Copeland, M.; Duchet, C.; Fabre P. *SPIE* **1989**, *1147*, 245.
(4) Du Lei, P.; Runt, J.; Savari, A.; Newman, R. E. *Macromolecules* **1987**, *20*, 1797.
(5) Kobayashi, T.; Minoshima, K.; Nomura, S.; Fukaya, S.; Ueki, A. *SPIE* **1989**, *1147*, 182.
(6) Möhlmann, R.; van der Vorst, C. P. J. M. in McArdle, C. B. *Side Chain Liquid Crystal Polymers*; Blackie, Glasgow, 1988; p 330.
(7) Singer, K. D.; Kuzyk, M. G.; Holland, W. R.; Sohn, J. E.; Lalama, J.; Commizzoli, R. B.; Katz, H. E.; Schilling, M. L. *Appl. Phys. Lett.* **1988**, *53*, 1800.
(8) Servay, Th.K.; Winkelhahn, L.; Schulze, M.; Böffel, C.; Neher, D.; Wegner, G. *Ber. Bunsen-Ges. Phys. Chem.* **1993**, *97*, 1272.
(9) Winkelhahn, H.-J.; Servay, Th.K.; Kalvoda, L.; Schulze, M.; Neher, D.; Wegner, G. *Ber. Bunsen-Ges. Phys. Chem.* **1993**, *97*, 1287.
(10) Heldmann, C.; Schulze, M.; Wegner, G. *Macromolecules* **1996**, *29*, 4686.
(11) Heldmann, C.; Neher, D.; Winkelhahn, H.-J.; Wegner, G. *Macromolecules* **1996**, *29*, 4697.
(12) Köhler, W.; Robello, D. R.; Dao, P. T.; Willand, C. S.; Williams, D. J. *J. Chem. Phys.* **1990**, *93*, 9157.
(13) Ulmann, A.; Willand, C.S.; Köhler, W.; Robello, D. R.; Williams, D. J.; Handley, L. *J. Am. Chem. Soc.* **1990**, *112*, 7083.
(14) Köhler, W.; Robello, D. R.; Willand, C. S.; Williams, D. J. *Macromolecules* **1991**, *24*, 4589.
(15) S'Heeren, G.; Persoons, A.; Bolink, H.; Heylen, M.; Van Beylen, M.; Samyn, C. *Eur. Polym. J.* **1993**, *29*, 981.
(16) Xu, C.; Wu, B.; Dalton, L. R.; Ranon, P. M.; Shi, Y.; Steier, W. H. *Macromolecules* **1992**, *25*, 6716.
(17) Xu, C. Z.; Wu, B.; Becker, M. W.; Dalton, L. R.; Ranon, P. M.; Shi, Y. Q.; Steier, W. H. *Chem. Mater.* **1993**, *5*, 1439.
(18) Zentel, R.; Baumann, H.; Scharf, D.; Eich, M.; Schoenfeld, A.; Kremer, F. *Makromol. Chem., Rapid Commun.* **1993**, *14*, 121.
(19) Lindsay, A.; Stenger-Smith, J. D.; Henry, R. A.; Hoover, J. M.; Nissan, R. A.; Wyne, K. *Macromolecules* **1992**, *25*, 6075.
(20) Levine, B. F.; Bethea, C. G. *J. Chem. Phys.* **1976**, *65*, 1989.
(21) (a) If the rods are nematic, the disordering possibilities are fewer (ultimately only up or down in the perfect nematic state) and order induced by the field is larger, up to ×5 in the perfect nematic state, less than this in practice. (b) Prasad, P. N.; Williams, D. J. *Introduction to Nonlinear Optical Effects in Molecules & Polymers*; John Wiley & Sons, Inc.: New York, 1991.
(22) Flory, P. J. *Principles of Polymer Chemistry*; Cornell University Press: Ithaca, NY, 1971.
(23) Gunn, J. M. F.; Warner, M. *Phys. Rev. Lett.* **1987**, *58*, 393.
(24) Warner, M. *MRS Proc.* **1989**, *134*, 61.
(25) Tsibouklis, J.; Richardson, P. H.; Ahmed, A. M.; Richards, R. W.; Feast, W. J.; Martin, S. J.; Bradley, D. D. C.; Warner, M. *Synthe. Met.* **1993**, *61*, 159.
(26) de Gennes, P-G. In *Polymer Liquid Crystals*; Ciferri, A.; Krigbaum, W. R.; Meyer, R. B. Eds.; Academic: New York, 1982.
(27) D'Allest, J. F.; Maissa, P.; ten Bosch, A.; Sixou, P.; Blumstein, A.; Blumstein, R.; Teixeira, J.; Noirez, L. *Phys. Rev. Lett.* **1988**, *61*, 2562.
(28) Naim, S. S.; Singh, S. K.; Sharma, S.; Gupta, S.; Fatma, N.; Chatterjee, R. K.; Katiyar, J. C. *Ind. J. Chem.* **1988**, *27B*, 1106.
(29) Fu, S.; Li, S.; Vogl, O. *Monatsh. Chem.* **1988**, *119*, 1299.
(30) Moore, J. S.; Stupp, S. I. *Macromolecules* **1990**, *23*, 65.
(31) Higashi, F.; Hoshito, A.; Yamada, Y.; Ozawa, M. *J. Polym Sci., Part A: Polym. Chem.* **1985**, *23*, 69.
(32) Teng, C. C.; Man, H. T. *Appl. Phys. Lett.* **1990**, *56*, 1734.
(33) van der Vorst, C. P. J. M.; van Weerdenburg, C. J. M. *SPIE* **1990**, *1337*, 246.
(34) Röhl, P.; Andress, B.; Nordmann, J. *Appl. Phys. Lett.* **1991**, *59*, 2793.
(35) Levy, Y.; Dumont, M.; Chastaing, E.; Robin, P.; Chollet, P. A; Gadret, G.; Kajzar, F. *Mol. Cryst. Liq. Cryst. Sci. Technol.* **1993**, *B4*, 1.
(36) Shuto, Y.; Amano, M.; Kano, T. *Jpn. J. Appl. Phys.* **1991**, *30*, 320.

MA971693F